J. Electroanal. Chem., 240 (1988) 77–87
Elsevier Sequoia S.A., Lausanne – Printed in The Netherlands

SCANNING TUNNELING MICROSCOPY (STM) AND SCANNING ELECTRON MICROSCOPY (SEM) OF ELECTRODISPERSED GOLD ELECTRODES

J. GÓMEZ, L. VÁZQUEZ and A.M. BARÓ

Dpto. de Física de Materia Condensada, C-III, Facultad de Ciencias, Universidad Autónoma de Madrid, Cantoblanco, 28049-Madrid (Spain)

C. ALONSO, E. GONZÁLEZ and J. GÓNZALEZ-VELASCO

Dpto. de Química (Lab. de Electroquímica), Facultad de Ciencias, Universidad Autónoma de Madrid, Cantoblanco, 28049-Madrid (Spain)

A.J. ARVÍA *

Instituto de Investigaciones Fisicoquímicas Teóricas y Aplicadas (INIFTA), Universidad Nacional de La Plata, Sucursal 4, Casilla de Correo 16, (1900) La Plata (Argentina)

(Received 13th February 1987; in revised form 6th August 1987)

ABSTRACT

Images of large active surface (electrodispersed) gold electrodes obtained by electroreduction of an oxide layer grown by applying a fast periodic square wave potential to polycrystalline specimens, have been obtained by STM and SEM. For the first time a correlation of imaging data of both microscopes can be established which allows one to find different structural details of these electrodes. The roughening increase produced by the electrochemical activation is explained tentatively through a generalized structural model consisting of an overlayer of sticking spheres of about 10 nm average diameter leaving inner interconnected channels of nearly the same average diameter and penetrating in the overlayer structure. The size of the spherical units is comparable to that of metal clusters involving the optimal ratio of surface to bulk atoms associated with the greatest catalytic activity.

INTRODUCTION

Gold electrodes of relatively large active surface area, i.e. electrodes involving roughness factors ranging from 10 to 10^3, can easily be obtained in acid electrolytes through a procedure involving the slow potentiodynamic electroreduction of a thick gold oxide layer formed previously by means of a periodic perturbing potential of

* Visiting Professor at the Universidad Autónoma de Madrid.

0022-0728/88/$03.50 © 1988 Elsevier Sequoia S.A.

well defined characteristics [1]. The electrode roughness, as compared to a mirror polished electrode of the same material, can be followed through the change in voltammetric charge corresponding to the O-adatom electrodesorption process by running a voltammogram in $HClO_4$ solution between -0.7 V and 1.1 V (vs. MSE) at 0.2 V/s. The kinetic behaviour of this type of electrode is very interesting in electrocatalysis, as has been demonstrated for platinum [2] for reactions such as H-adatom electroadsorption–electrodesorption and reduced CO_2 electrooxidation in acids. For roughness factors up to about 10^3 and under conventional voltammetric conditions, these treated platinum electrodes behave as practically ideal electrodispersed platinum electrodes.

Recently, STM imaging [3,4] has been applied successfully as an ex-situ technique for investigating two differently treated electrodes, namely, the topography and the structure at the subnanometer level of large active surface area platinum electrodes [5] and stepped and preferred oriented platinum surface structures [6,7]. In the former case the structure of large area platinum electrodes consists of a large number of sticking metal clusters. The utmost importance of these problems in heterogeneous catalysis requires further investigations with other metals to improve the original model and to test its general validity [5].

The present paper is devoted to the study of the topography of electrodispersed gold electrodes using SEM at a relatively low resolution to avoid surface damage and by means of STM to discover new topographic details at the subnanometer scale. Imaging in the whole range furnishes very interesting and complementary information on the structure of this type of large active surface area electrodes which can be correlated with some basic catalytic properties of highly dispersed metals.

EXPERIMENTAL

The working electrode was prepared from a polycrystalline gold wire 0.5 mm thick, 99.99% purity, according to the following procedure: (i) Formation of a gold sphere (about 0.2 mm dia.) by melting one end of the wire in an oxygen–gas flame and immediately cooling in distilled water. (ii) Potentiodynamic cycling in 1 *M* $HClO_4$ at 0.2 V/s between -0.7 V and 1.1 V (vs. $Hg/Hg_2SO_4/1$ *M* K_2SO_4 reference electrode) (MSE), to obtain the stabilized voltammogram (blank). (iii) Repetitive square wave potential scanning (RSWPS) applied to the electrode in the same solution at 4 kHz between -0.045 V (MSE) and 2.045 V (MSE) for a time going from 1 to 3 min to form a thick hydrous gold oxide layer. In this case τ_u and τ_l, the positive and negative half-cycle times, were 0.15 ms and 0.10 ms, respectively. The RSWPS treatment was interrupted at 2.045 V. (iv) The anodic layer prepared through the RSWPS treatment was electroreduced by means of a linear potential sweep at 0.01 V/s, to -0.7 V. At this stage the electrodispersed gold electrode is obtained. (v) Finally, the changes in the electrochemical properties of the new metal surfaces were followed voltammetrically in 1 *M* $HClO_4$, in the same way as for the blank.

The operating procedure was performed at 25°C using a conventional three compartment cell with an electrode arrangement involving negligible ohmic polarization. The circuitry involved a gold working electrode, a gold counterelectrode immersed in a cell compartment separated by a fritted glass disc, and a MSE placed into a compartment connected to the rest of the cell through a Luggin–Haber capillary tip. The electrolyte solution (1 *M* $HClO_4$) was made from Milli-Q# water and 71% $HClO_4$ (a.r. Merck). The basic electronic equipment for the electrochemical measurements consisted of a Brucker model 310 potentiostat and a PAR function generator model 175.

Ex-situ SEM micrographs of the different specimens were obtained under the usual vacuum conditions using a Philips 500 scanning electron microscope. The currents at the samples were no greater than 10^{-11} A to exclude surface damage. This was checked, particularly at the largest SEM magnification, through the reproducibility of the voltammograms of the specimen in $HClO_4$ solution before and after the SEM imaging.

Ex-situ STM imaging of blank and treated gold electrodes was performed in air. The microscope used was of the so-called pocket size type which uses a stack of metal plates separated by viton spacers to absorb external mechanical vibrations [8]. Data were taken at several tunneling voltages (tip positive) and a tunneling current of 10 μA. The scanning frequency was placed at 0.1 Hz.

The images were obtained by plotting the voltage applied to the tip piezodrives on a X–Y recorder. At the same time the data were acquired with a DACA card installed on a IBM PC-AT and stored on a hard disc in order to be processed subsequently. Data processing consisted of the following steps: (i) Treatment of the data with a smoothing filter; (ii) removal of a background plane to eliminate the lack of perpendicularity between the sample and the tip; (iii) image processing. The processed images were displayed essentially in two different ways, namely, a three-dimensional display taken with any orientation, in particular 90° (top view) and illuminated laterally, and a contour map of equal corrugation lines or its equivalent using a color or gray scale. The images could be rotated around the z-axis by any angle in order to make apparent hidden features [9].

RESULTS

Voltammetric data. Evaluation of the electrode roughness

The voltammogram of the blank and those of treated gold electrodes (Fig. 1) run in 1 *M* $HClO_4$ at 0.2 V/s in the potential range of the thermodynamic stability of bulk water, are of comparable shape, except for the current scaling factor and the distribution of peaks which are referred to further on. These results are similar to those already reported in the literature for bright gold electrodes in the same acid solution [8]. Thus, both voltammograms present a complex anodic charge contribution in the 0.6 V to 1.1 V range related to the electroformation of the O-containing surface species, and a well-defined electroreduction current peak extending from

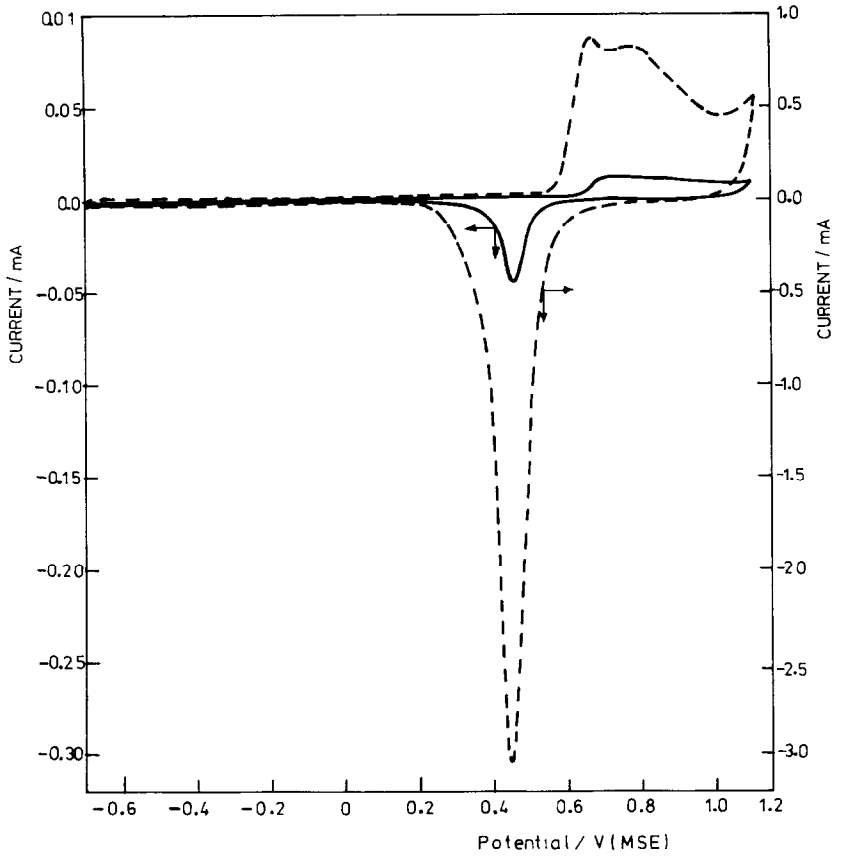

Fig. 1. Voltammograms at 0.2 V/s of a gold electrode in 1 M $HClO_4$ at 25 °C. The solid line corresponds to the blank and the dashed line to an activated gold electrode with $R = 83$.

about 0.6 V to about 0.2 V, which corresponds to the complementary electroreduction reaction.

The voltammetric charge is obviously increased for those electrodes which were prepared by electroreduction of the oxide layer formed through the RSWPS treatment. On the basis that the same surface reaction takes place on both blank and treated electrode, the relative increase in active surface area can be given in terms of a roughness factor, R, defined as the ratio of the voltammetric electroreduction charge of the treated gold electrode to that of the blank. For the present work the value of R increases according to the duration of the RSWPS treatment. In this way values of R ranging from 5 up to about 200 were obtained.

A more detailed analysis of the voltammogram shape shows that the distribution of the anodic peak fine structure is somewhat different for the treated electrodes

and for the blank. Each anodic peak has been assigned to the formation of O-containing surface species taking place at a different crystallographic face of the polycrystalline gold surface [10]. The voltammogram shows that the increase in roughness obtained by electroreduction of the oxide layer after the RSWPS treatment produces a change in the distribution of crystallographic faces, namely the treated gold electrode exhibits a specific preferred crystallographic orientation [11].

SEM micrographs

The SEM micrograph of the blank (Fig. 2a), that is the mirror polished polycrystalline gold electrode surface which was subjected to a repetitive voltammetric scan at 0.2 V/s between −1.7 V and 1.1 V in order to obtain the corresponding stabilized voltammogram, shows a relatively rough surface with rounded clusters of about 10 μm average diameter which in part coalesce to form larger clusters with

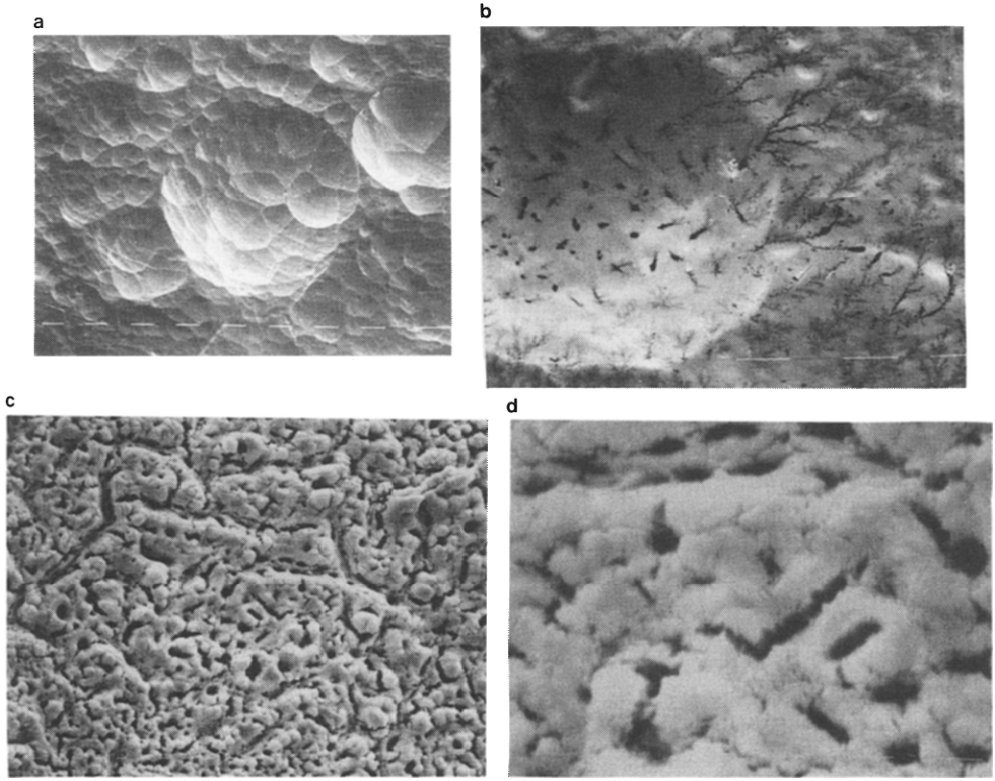

Fig. 2. SEM micrographs of gold electrodes, (a) Blank, 260×; (b) $R = 10$, 600×; (c) $R = 120$, 1200×; (d) $R = 120$, 4800×.

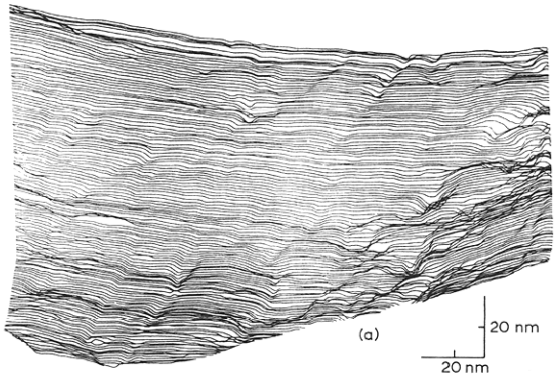
(a)
20 nm
20 nm

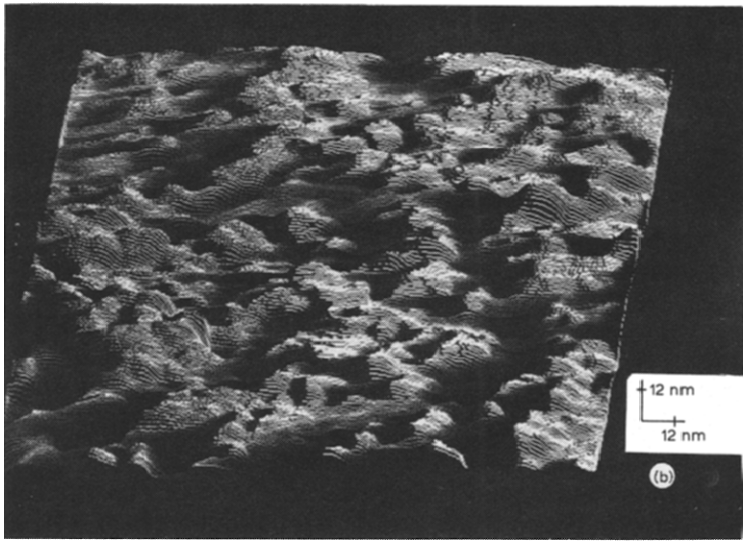
12 nm
12 nm
(b)

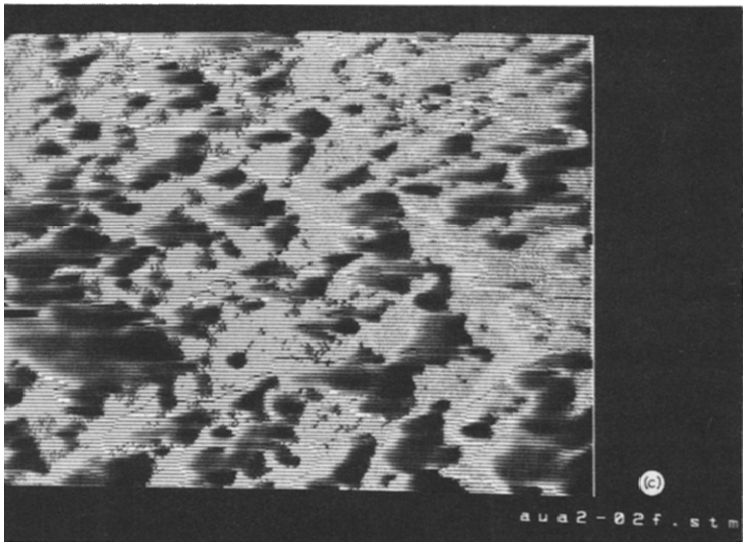
(c)
aua2-02f.stm

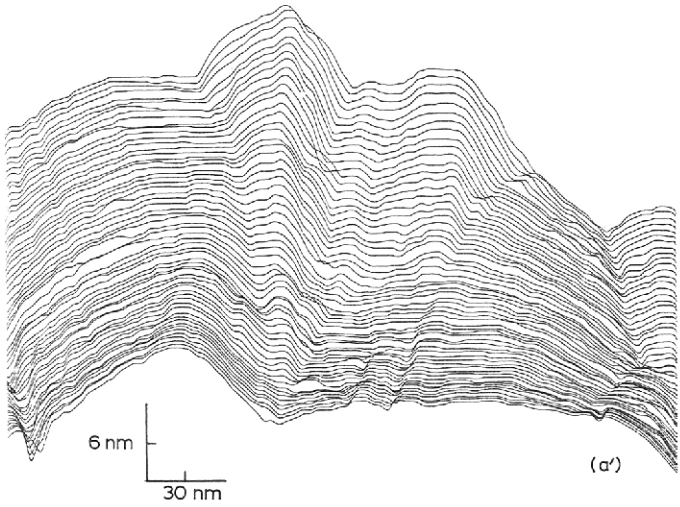

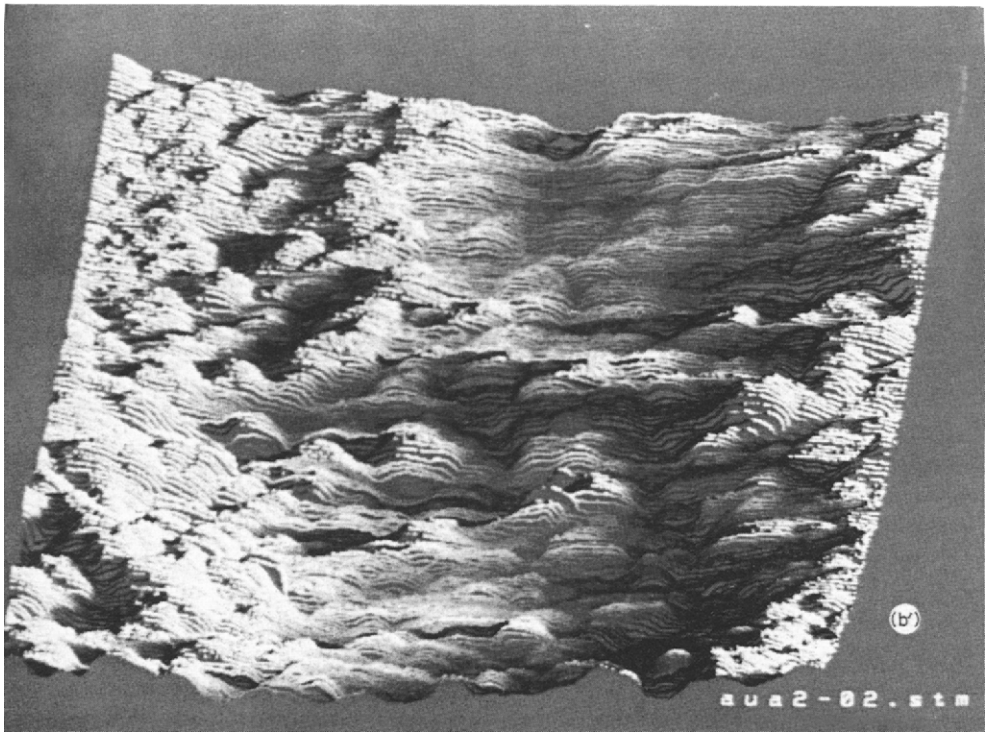

Fig. 3. (a) STM image taken with an X–Y recorder of an $R = 30$ activated gold surface. Two main features can be seen; (i) oriented steps aligned mainly in one direction; (ii) a rough surface showing some rounded features about 10 nm in diameter. (a′) STM image of the untreated mirror gold surface (blank). (b) STM 3-D processed image illuminated laterally from an $R = 80$ activated gold surface. The surface is now rough and full of rounded domes of about 10 nm diameter. (b′) Same as (b) without smoothing. (c) Same as (b) but seen from the top. The processed image makes clearer the orientation of the domes and the size of some features.

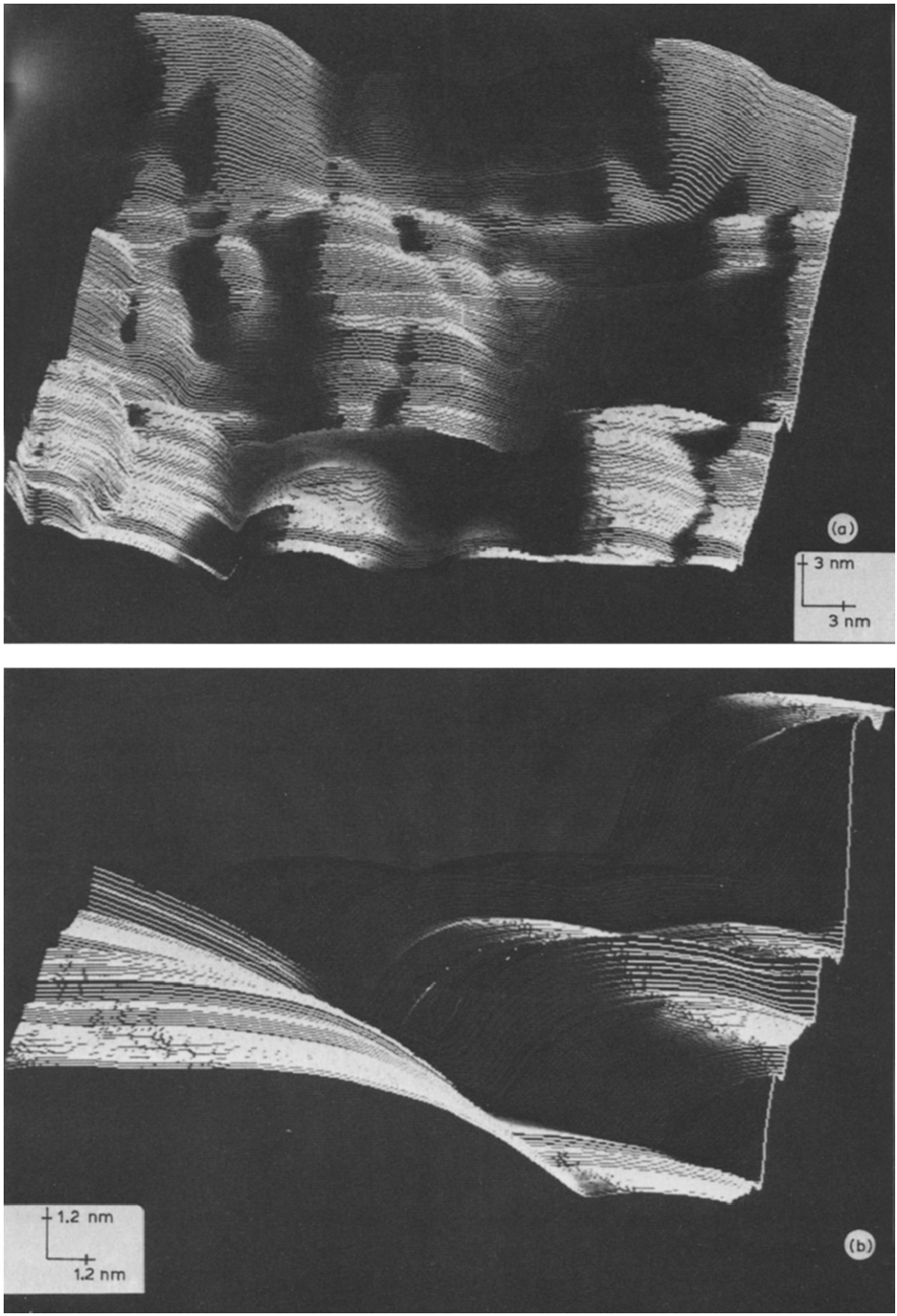

Fig. 4. (a) STM 3-D view of the $R = 80$ activated gold surface taken at a higher sensitivity. (b) Further magnification of the $R = 80$ activated gold surface. The flatness of the structure can be seen clearly.

the appearance of a cauliflower structure. The roughness factor of this electrode surface as compared to that of the initial untreated mirror surface is about 6.

The topography described above disappears gradually following the RSWPS treatment, and correspondingly R increases (Fig. 2b) and the cauliflower structure is replaced by a new one consisting of sponge-like globules with small irregular channels and long multiple branched channels interconnecting different globules. This new heterogeneous topography extends over the whole electrode surface when the value of R is greater than 100 (Fig. 2c). Then, the primitive topography is no longer observed and at larger magnification (Fig. 2d) the solid region in the small globules consists of a larger number of uniformly distributed small pores.

STM imaging

STM images for $R = 30$ obtained directly with an X–Y recorder (Fig. 3a) show a heterogeneous surface with two different topographies, namely a relatively flat region with steps of about 1.5 nm height and another consisting of domes of about 10 nm average diameter. The rough topography definitely prevails for $R = 80$, maintaining the same average diameter for the domes (Fig. 3b). A top view image of Fig. 3b (Fig. 3c) shows the existence of some orientation in the structure. At least two well defined directions forming an angle close to 90° can be recognized and these can be correlated with the observation of preferred crystallographic orientation derived from the voltammogram fine structure. Similar features were also observed for electrodispersed platinum electrodes [5].

In order to look at the domed structure, images at a higher sensitivity were obtained. The amplified image of an electrodispersed gold electrode surface (Fig. 4a) shows clearly the growing process of the spheres. Further magnification (Fig. 4b) displays the boundaries between different spheres in the form of flat channels, whose average diameter is comparable to that of the spheres. In addition the surface fine structure of the spheres can be measured; they show a remarkable flatness with a corrugation below 0.1 nm.

DISCUSSION

STM and SEM images give, for the first time, topographic details of an electrodispersed gold electrode which nearly cover the range from normal dimensions to the subnanometer scale. The results show that the topography of these electrodes is comparable to that described recently for electrodispersed platinum electrodes [5], that is, the structure of the electrode is heterogeneous and corresponds to proportions of rough/smooth surface which are not uniform over the entire electrode. Therefore, one can conclude that the metal structure resulting from slow electroreduction of the oxide layer formed under relatively fast RSWPS conditions is independent of the nature of the electrode, at least for platinum and gold.

At low resolution sponge-like globules at the μm level involving large steps and

branched channels are observed. At high resolution the topography shows corrugated regions and regions made of small adhering sphere-like pieces of 10 nm average diameter. The small spheres are separated by channels whose average diameter is about the same as that of the spheres themselves. These regions are the major cause of the real increase in the electrode surface area [5]. The contribution of the corrugated structure to the roughness increase cannot explain the large values of R observed. In this sense STM data provide a way to calculate the real area of the electrodispersed electrodes. Such calculations show that the area increase due exclusively to surface corrugations is not higher than 15% [12].

The increase in real surface area can be explained through a model consisting of a metal overlayer made of small adhering spheres of about 10 nm diameter [5]. This model is consistent with the R factor measured from voltammetric data, if one assumes that the metal overlayer volume is equal to the apparent electrode surface area times the thickness of the overlayer as deduced from the oxide layer electroreduction charge.

Now as far as the behavior of the small spheres is concerned, it should be noted that chemisorbed reactants such as adsorbed atoms or radicals on metals are sensitive to the particle size of the electrocatalyst [13]. Reaction behavior as a function of sites with low coordination numbers such as edges or kinks on the crystallites has been examined by varying the crystallite size. In fact, smaller particles (2–5 nm in size) exhibit a remarkable selectivity for certain reactions related principally to the ratio of atoms at the surface to atoms in the bulk. Thus, for a sphere of 10 nm diameter, the maximum number of atoms of about 0.28 nm diameter, such as Pt or Au, is about 3×10^4, out of which about 3×10^3 atoms lie on the sphere surface. Nevertheless, for this particular cluster size the overlapping of electron clouds between atoms located at opposite surface positions becomes negligible. Hence, the properties of these metal clusters should, in principle, be close to those of the bulk metal. Therefore, it appears that the structure acquired by the active surface electrode involves the minimum size of the spheres which is compatible with the macroscopic properties of the metal. This is in agreement with the fact that there are no major changes in the voltammogram for the electrodispersed treatment as compared to the blank. Furthermore, for 10 nm diameter spheres involving incomplete cubo-octahedrons the ratio between the number of atoms at the surface and in the sphere bulk is close to that of crystallites exhibiting the greatest activity for various gas-phase catalytic reactions and electrochemical heterogeneous reactions [14–18].

The high resolution STM image processing also provides, to a certain degree, a clear demonstration of preferred crystallographic orientation at the surface of the gold spheres. This result confirms that the increase in electrode area is accompanied by a simultaneous electrochemical faceting, as can be also deduced from voltammetry.

In summary, a definite correlation between the SEM and STM microscopic data and voltammetry for electrodispersed gold electrodes has been accomplished. The structural model derived from STM data for electrodispersed platinum and gold

electrodes furnishes a reasonable explanation for their remarkable increase in active surface area.

ACKNOWLEDGEMENTS

The authors are indebted to J. Presa, M.A. Béjar and J.M. Gómez-Herrero for help on the image processing of STM data and to A. Bartolomé for assistance in the experiments. Financial support from CAICyT under contract No. 0386/84 is gratefully acknowledged.

REFERENCES

1 A.C. Chialvo, W.E. Triaca and A.J. Aivía, J. Electroanal. Chem., 171 (1984) 303.
2 S.M. Piovano, A.C. Chialvo, W.E. Triaca and A.J. Arvia, J. Appl. Electrochem., 17 (1987) 147.
3 G. Binnig and H. Röhrer, Helv. Phys. Lett., 55 (1982) 726; Surf. Sci., 126 (1983) 236.
4 G. Binnig and H. Röhrer, Sci. Am., 253 (1985) 50.
5 L. Vázquez, J. Gómez, A.M. Baró, N. García, M.L. Marcos, J. González Velasco, J.M. Vara, A.J. Arvía, J. Presa, A. García and M. Aguilar, J. Am. Chem. Soc., 109 (1987) 1730.
6 J. Gómez, L. Vázquez, A.M. Baró, C.L. Perdriel, W.E. Triaca and A.J. Arvía, Nature (London), 323 (1986) 612.
7 L. Vázquez, J.M. Gómez Rodríguez, J. Gómez Herrero, A.M. Baró, N. García, J.C. Canullo and A.J. Arvía, Surf. Sci., in press.
8 C.M. Ferro, A.J. Calandra and A.J. Arvía, J. Electroanal. Chem., 55, 291 (1974).
9 M.A. Béjar, J. Gómez-Herrero and A.M. Baró, unpublished results, 1986.
10 G.J. Brug, M. Sluyters-Rehbach, J.H. Sluyters and A. Hamelin, J. Electroanal. Chem., 181 (1984) 245.
11 C.L. Perdriel, M. Ipohorski and A.J. Arvía, J. Electroanal. Chem., 215 (1986) 317.
12 J. Presa, unpublished work, 1986.
13 P. Stonehart, K. Konoshita and J.A.S. Bett in M. Breiter (Ed.), Proceedings of Electrocatalysis, The Electrochemical Society, Princeton, 1974, p. 275.
14 O.M. Poltorak and V.S. Boronin, Russ. J. Phys. Chem., 40 (1966) 1436.
15 J. Lundquist and P. Stonehart, Electrochim. Acta, 18 (1973) 349.
16 P. Stonehart, H.A. Kozlowska and B.E. Conway, Proc. R. Soc. Ser. A, 310 (1969) 541.
17 G.R. Wilson and W.K. Hall, J. Catal., 17 (1970) 190; 24 (1972) 306.
18 J. Freel, J. Catal., 25 (1972) 149.